

# UC San Francisco

## UC San Francisco Previously Published Works

### Title

Spinal cord gray matter atrophy correlates with multiple sclerosis disability

### Permalink

<https://escholarship.org/uc/item/4700h2qr>

### Journal

Annals of Neurology, 76(4)

### ISSN

0364-5134

### Authors

Schlaeger, R  
Papinutto, N  
Panara, V  
[et al.](#)

### Publication Date

2014-10-01

### DOI

10.1002/ana.24241

Peer reviewed

# Spinal Cord Gray Matter Atrophy Correlates with Multiple Sclerosis Disability

Regina Schlaeger, MD,<sup>1,2</sup> Nico Papinutto, PhD,<sup>1</sup> Valentina Panara, MD,<sup>1,3</sup>  
 Carolyn Bevan, MD,<sup>1</sup> Iryna V. Lobach, PhD,<sup>1</sup> Monica Bucci, MD,<sup>1</sup>  
 Eduardo Caverzasi, MD,<sup>1</sup> Jeffrey M. Gelfand, MD, MAS,<sup>1</sup>  
 Ari J. Green, MD, MCR,<sup>1,4</sup> Keshi M. Jordan, BS,<sup>1,5</sup> William A. Stern, RT,<sup>1</sup>  
 H.-Christian von Büdingen, MD,<sup>1</sup> Emmanuelle Waubant, MD, PhD,<sup>1</sup>  
 Alyssa H. Zhu, MSc,<sup>1</sup> Douglas S. Goodin, MD,<sup>1</sup>  
 Bruce A. C. Cree, MD, PhD, MCR,<sup>1</sup> Stephen L. Hauser, MD,<sup>1</sup> and  
 Roland G. Henry, PhD<sup>1,5,6</sup>

**Objective:** In multiple sclerosis (MS), cerebral gray matter (GM) atrophy correlates more strongly than white matter (WM) atrophy with disability. The corresponding relationships in the spinal cord (SC) are unknown due to technical limitations in assessing SC GM atrophy. Using phase-sensitive inversion recovery (PSIR) magnetic resonance imaging, we determined the association of the SC GM and SC WM areas with MS disability and disease type.

**Methods:** A total of 113 MS patients and 20 healthy controls were examined at 3T with a PSIR sequence acquired at the C2/C3 disk level. Two independent, clinically masked readers measured the cord WM and GM areas. Correlations between cord areas and Expanded Disability Status Score (EDSS) were determined. Differences in areas between groups were assessed with age and sex as covariates.

**Results:** Relapsing MS (RMS) patients showed smaller SC GM areas than age- and sex-matched controls ( $p = 0.008$ ) without significant differences in SC WM areas. Progressive MS patients showed smaller SC GM and SC WM areas compared to RMS patients (all  $p \leq 0.004$ ). SC GM, SC WM, and whole cord areas inversely correlated with EDSS ( $\rho: -0.60, -0.32, -0.42$ , respectively; all  $p \leq 0.001$ ). The SC GM area was the strongest correlate of disability in multivariate models including brain GM and WM volumes, fluid-attenuated inversion recovery lesion load, T1 lesion load, SC WM area, number of SC T2 lesions, age, sex, and disease duration. Brain and spinal GM independently contributed to EDSS.

**Interpretation:** SC GM atrophy is detectable in vivo in the absence of WM atrophy in RMS. It is more pronounced in progressive MS than RMS and contributes more to patient disability than SC WM or brain GM atrophy.

ANN NEUROL 2014;76:568–580

The involvement of the spinal cord gray matter (GM) in multiple sclerosis (MS) was recognized during the late 19th and early 20th century.<sup>1–4</sup> In 1933, Davison described various changes in the anterior horn cells

View this article online at [wileyonlinelibrary.com](http://wileyonlinelibrary.com). DOI: 10.1002/ana.24241

Received Mar 7, 2014, and in revised form Jul 25, 2014. Accepted for publication Jul 28, 2014.

Address correspondence to Dr Henry, Director, Imaging in Multiple Sclerosis, Department of Neurology, University of California, San Francisco, 675 Nelson Rising Lane, Box 3206, San Francisco, CA 94158. E-mail: [Roland.Henry@ucsf.edu](mailto:Roland.Henry@ucsf.edu)

From the <sup>1</sup>Department of Neurology, University of California, San Francisco, San Francisco, CA; <sup>2</sup>Department of Neurology, University Hospital Basel, University of Basel, Basel, Switzerland; <sup>3</sup>Institute of Advanced Biomedical Technologies, University "G. D'Annunzio," Chieti, Italy; <sup>4</sup>Department of Ophthalmology, University of California, San Francisco, San Francisco, CA; <sup>5</sup>Bioengineering Graduate Group, University of California, San Francisco, San Francisco and University of California, Berkeley, Berkeley, CA; and <sup>6</sup>Department of Radiology and Biomedical Imaging, University of California, San Francisco, San Francisco, CA.

Additional supporting information can be found in the online version of this article.

(shrinkage, pyknosis, central chromatolysis, swelling, vacuolization) as well as pronounced gliosis of the spinal cord GM.<sup>5</sup> This corresponded to clinically documented muscular atrophy (especially in the intrinsic hand muscles) in the majority of MS cases assessed at autopsy.<sup>5</sup> Involvement of myelinated axons within the GM is also a well-established feature of MS pathology; demyelination of these axons was first reported by Dawson in 1916.<sup>6</sup> However, following these early insights, the attention of the scientific community shifted away from the GM pathology in MS. For several decades thereafter, MS was generally regarded as a white matter (WM) disease. The development of modern myelin immunohistochemical stains, which enabled improved detection of cortical MS lesions, promoted a renewed interest in GM pathology in MS.<sup>7-9</sup> Since that time, cortical GM pathology and its clinical impact on MS have been extensively studied both in vivo and ex vivo (reviewed by Geurts et al<sup>10</sup>). However, few reports have focused on involvement of spinal cord GM in MS.

In one postmortem study, Gilmore and coworkers reported that approximately 50% of the spinal cord GM was demyelinated in patients with progressive MS, suggesting that the extent of demyelination in the GM exceeded that present in the WM of the spinal cord by about one-third.<sup>11</sup> This same group also reported that both the total neuronal cell count and the interneuronal cross-sectional area were reduced in the upper cervical levels of MS patients.<sup>12</sup> Nevertheless, the reported volumetric histopathological data on the extent of WM and GM atrophy in the spinal cord in MS are conflicting. Some authors observed a similar reduction of both GM and WM cross-sectional cervical cord areas in advanced progressive MS (with a trend toward a predominance of GM loss),<sup>13</sup> whereas others reported significant WM loss without GM loss.<sup>14</sup>

Until recently, the lack of sufficient spatial resolution and the poor contrast between GM and WM on conventional magnetic resonance imaging (MRI) and their susceptibility to motion and other artifacts have hampered in vivo assessment of spinal cord GM.<sup>15</sup>

T2\*-weighted imaging has been recently used to assess spinal cord WM and GM compartments in healthy controls.<sup>16,17</sup> The introduction of phase-sensitive inversion recovery (PSIR) imaging<sup>18,19</sup> offers another promising approach to overcome several of these technical challenges.<sup>20,21</sup> A novel 2-dimensional (2D) optimized PSIR protocol has enabled sensitive and clinically feasible spinal cord imaging of GM atrophy (SF-SIGMA) in efficient acquisition times of 2 minutes with reliable GM and WM area measurements.<sup>22</sup>

Here we report the associations of the cervical spine GM with MS disability and disease progression in a large

single-center cross-sectional MS cohort using PSIR imaging.

## Subjects and Methods

### Research Participants

The Committee on Human Research at the University of California, San Francisco (UCSF) approved the study protocol. Written informed consent was obtained from all participants. A total of 127 patients seen at the UCSF Multiple Sclerosis Center between July 2013 and October 2013 as part of an ongoing observational study were screened for participation. Inclusion criteria were: (1) a diagnosis of MS according to international panel criteria<sup>23</sup> and (2) age  $\geq$  18 years. Exclusion criteria were: (1) relapses within 4 weeks prior to the visit; (2) use of corticosteroids within 4 weeks prior to the MRI examination; (3) a recent history or suspicion of current drug or alcohol abuse; (4) a diagnosis of hepatitis B or C or human immunodeficiency virus; (5) participation in ongoing MS trials with unlicensed drugs; (6) any concurrent illness, disability, or clinically significant abnormality (including laboratory tests) that would prevent the subject from safely completing the assessments, such as metallic objects on or inside the body; and (7) distortion of the PSIR image at the intervertebral disk level of C2/C3, making the delimitation of GM and WM impossible. This latter point led to exclusion of 14 of 127 screened patients (11%). In 5 patients with progressive forms of MS and in 9 patients with relapsing MS (RMS), delimiting the spinal cord GM was impossible due to motion artifacts or extensive lesions. Twenty healthy control subjects, selected to best match the RMS group regarding age and sex distributions, were also included.

### Clinical Assessments

All patients received a standardized clinical neurological examination including Neurostatus Expanded Disability Status Score (EDSS), Timed 25-Foot Walk Test (T25W), and 9-Hole Peg Test (9HPT).<sup>24-26</sup>

### Image Acquisition

All subjects were scanned on a Siemens (Erlangen, Germany) 3T Skyra scanner with a 20-channel neck-head coil and a 32-channel spine coil within 2 weeks of their clinical examination. Axial 2D-PSIR images were acquired perpendicular to the spinal cord at the C2/C3 intervertebral disk level (Fig 1) with a total scan time of <2 minutes. Acquisition parameters were as follows: in-plane resolution =  $0.78 \times 0.78\text{mm}^2$ , slice thickness = 5mm, matrix  $256 \times 256$ , repetition time (TR) = 4,000 milliseconds, echo time (TE) = 3.22 milliseconds, inversion time (TI) = 400 milliseconds, angle =  $10^\circ$ , 3 averages. To minimize neck movement during the examination, each subject was provided with an MRI-compatible cervical collar,<sup>16</sup> and special care was taken to position the patient comfortably.

In addition, the participants underwent a standard high-resolution T1-weighted image of the brain (magnetization prepared rapid acquisition gradient echo [MPRAGE], sagittal acquisition,  $1\text{mm}^3$  cubic voxel, TR = 2,300 milliseconds, TE = 2.98 milliseconds, TI = 900 milliseconds, angle  $9^\circ$ ),

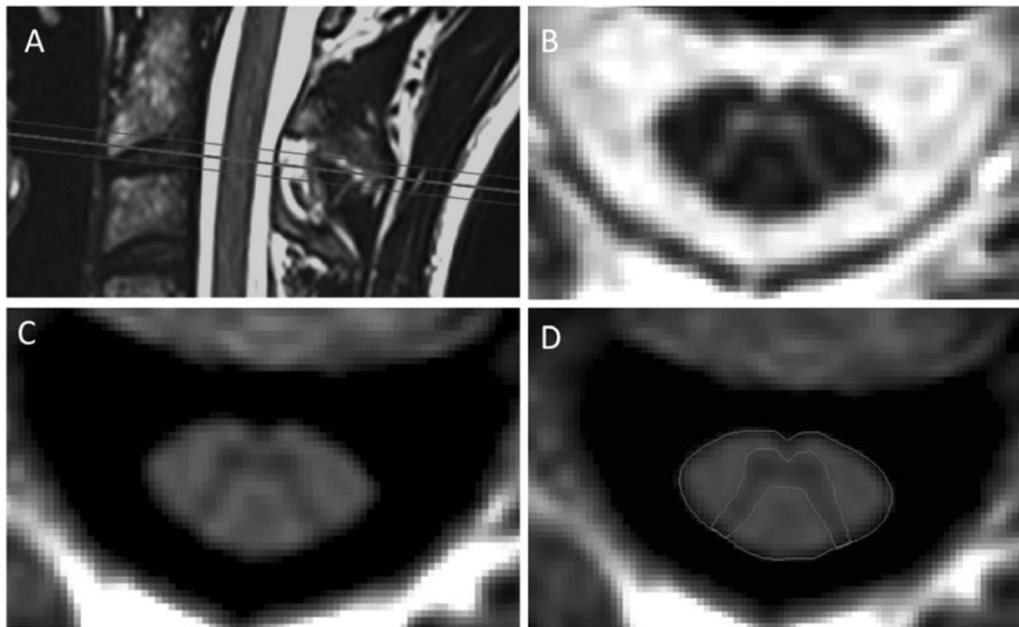


**FIGURE 1:** (A–D) Axial 2-dimensional phase-sensitive inversion recovery (PSIR; C) and magnitude (B) images were acquired at the C2/C3 disk level perpendicular to the cord (A). Segmentation of the cord area was conducted semiautomatically using an active surface model. Segmentation of the gray matter area was performed manually on the PSIR image (D). Images are from a healthy control.

a 3D fluid-attenuated inversion recovery (FLAIR) of the brain (sagittal acquisition,  $1\text{mm}^3$  cubic voxel, TR = 5,000 milliseconds, TE = 389 milliseconds, TI = 1,800 milliseconds), and standard T2-weighted sagittal images of the cervical cord ( $0.72 \times 0.72\text{mm}^2$ , slice thickness = 1.2mm, field of view [FOV] =  $230 \times 230\text{mm}^2$ , TR = 5,280 milliseconds, TE = 85 milliseconds) and thoracic cord ( $0.68 \times 0.68\text{mm}^2$ , slice thickness = 2mm, FOV =  $300 \times 300\text{mm}^2$ , TR = 4,290 milliseconds, TE = 90 milliseconds), as well as T2-weighted axial images of the cervical cord ( $0.62 \times 0.62\text{mm}^2$ , slice thickness = 3mm, TR = 4,000 milliseconds, TE = 92 milliseconds).

### Image Analysis

Two readers, one neuroradiologist (V.P.) and one MS neurologist (R.S.), who were both masked to the clinical information, independently assessed the upper cervical cord area (UCCA) and the spinal cord GM area at the intervertebral disk level of C2/C3 on the phase-sensitive reconstructed images (Fig 1) using the software JIM6 (Xinapse Systems, www.xinapse.com). Both readers performed their assessment on the same workstation. The UCCA measurement was semiautomated.<sup>27</sup> The GM area was manually segmented  $3\times$  by each reader, and the mean GM area was calculated per reader. The spinal cord WM area was measured as the difference between the UCCA and GM areas for each reader. An experienced MS neuroradiologist (M.B.), who was masked to both clinical information and the PSIR images, performed the spinal cord lesion count on the T2-weighted images. Cortical reconstruction and segmentation of the cerebral MPRAGE data sets were performed with the FreeSurfer image analysis suite (available for download at <http://surfer.nmr.mgh.harvard.edu/>), and normalized brain GM

and WM volumes, and brain T1 lesion load were determined. FLAIR lesion loads were measured through a semiautomatic procedure using AMIRA 5.4 (Mercury Computer Systems, Chelmsford, MA).

### Statistical Analyses

Intraclass correlation coefficients (ICCs) were calculated to assess intra- and inter-rater reliability of the GM area measurements and inter-rater reliability of the semiautomated UCCA measurements of the whole cohort.

The relationships between the PSIR measures (UCCA, mean GM, and mean WM areas) and the clinical measures (EDSS, T25W, and 9HPT) were assessed using a Spearman rank correlation. Linear regression analysis was used to assess differences in PSIR measures between controls, RMS, and progressive patients, as well as between controls, progressive patients, and those who fulfilled proposed criteria for a benign/mild disease course<sup>28</sup> (as defined by a minimum disease duration of 15 years and an EDSS  $\leq 2.5$ ).<sup>24</sup> This analysis was first performed with age and sex and secondly (for patients only) with disease duration and sex as covariates. These assessments were made using the mean values across both readers' measurements, and then those of each reader separately to assess variability.

The relationship between spinal cord GM area and normalized brain GM volume was assessed using Pearson correlation. The relationship between spinal cord areas and the number of spinal cord lesions was assessed by Spearman rank correlation (given the non-normal distribution of the number of spinal cord lesions).

Regression subset selection, including exhaustive search (LEAPS<sup>29</sup> package in R [R Foundation, <http://www.r-project>].

org]) modeling and analyses of relative importance of regressors in a linear model (RELAIMPO package in R),<sup>30,31</sup> was used to analyze the relative contribution of spinal cord GM area to MS disability (as measured by EDSS), along with other variables of potential interest (normalized brain GM volume, normalized brain WM volume, brain T1 lesion volume, brain FLAIR lesion volume, spinal cord WM area, number of spinal cord T2 lesions, age, sex, and disease duration) in the context of inter-correlations between variables. The resulting largest model including all variables is referred to as Model 1. As the variable *number of spinal cord T2 lesions* was not normally distributed, we also performed a sensitivity analysis including the variable *logarithmic transformed number of spinal cord T2 lesions* into the model, which provided very similar results.

To determine the significance of the differences between the relative contributions of the spinal cord GM area and the other MRI variables to MS disability, we performed a bootstrapping with 1,000 iterations and calculated the respective confidence intervals (CIs) of these differences.

Because the LEAPS analysis indicated that spinal cord and brain GM were the strongest predictors of EDSS, we calculated the diagnostic likelihood ratio (DLR)<sup>32</sup> to estimate the covariate-adjusted risk imparted by each of these variables to improve the likelihood of a correct classification of a progressive versus relapsing and of a progressive versus mild disease course. Calculation of the DLR was based on binary logistic regression with disease type (progressive vs relapsing or vs mild, respectively) as outcome variables<sup>32</sup> as implemented in the R package DTComPair. The risk for each subject was estimated as the probability of being progressive based on a normalized brain GM model, a spinal cord GM model, and a combined model including both brain and spinal cord GM.

The DLRs were determined from the differences between the combined model and the individual models, and testing for significance in the DLR was performed for the addition of brain and the addition of spinal cord using the DTComPair package in R based on the Gu formulas.<sup>32</sup>

Receiver operating characteristic (ROC) curves were determined to assess sensitivity and specificity for the prediction of a progressive disease course given by the binary logistic models based on either brain GM volume or spinal cord GM area, and the respective areas under the curve were calculated.

Statistical analysis was performed using SPSS Statistics v21 (IBM, Armonk, NY), JMP Statistics (www.jmp.com) v11 (SAS Institute, Cary, NC), and R.

## Results

Patients' clinical characteristics are described in Table 1. A total of 113 MS patients were included: 88 patients with RMS disease course and 25 with a progressive MS (18 with secondary progressive, 6 with primary progressive, and 1 with progressive relapsing MS). In the RMS group, 31.8% (28 of 88) fulfilled proposed criteria for a benign/mild disease course.<sup>28</sup> As expected, patients with RMS had a significantly lower age and shorter disease duration than those with progressive MS.

The control group showed similar distributions of age and sex compared to the RMS patients. Controls had a mean age of 48.6 years (median = 48.0, standard deviation = 12.24); 12 were women, and 8 were men.

The site for assessment of the cervical cord area (at the C2/C3 intervertebral disk level) was chosen because

**TABLE 1. Patient Characteristics**

Characteristic	Progressive MS	Relapsing MS	Mild MS (subgroup of RMS) <sup>a</sup>
No.	25	88	28
Subtype	6 PPMS, 18 SPMS, 1 PRMS		
Age, yr			
Mean ± SD	57.3 ± 10.5	48.8 ± 9.4	55.3 ± 8.9
Q1/median/Q3	46.6/58.0/63.6	42.1/48.2/55.2	50.8/57.4/61.4
Gender, F/M	12/13	55/33	17/11
Disease duration, yr			
Mean ± SD	20.0 ± 11.4	15.3 ± 8.7	22.9 ± 7.9
Q1/median/Q3	13.6/17.5/26.8	10.5 /13.0/18.5	17.7/19.8/24.5
EDSS			
Q1/median/Q3	4.0/6.0/6.5	1.5/2.0/2.5	1.5/1.5/2.0
Range	2.0–8.0	0–5.0	0–2.5

<sup>a</sup>Mild MS is defined as EDSS ≤ 2.5 and disease duration > 15 years.  
 EDSS = Expanded Disability Status Score; F = female; M = male; MS = multiple sclerosis; PPMS = primary progressive MS; PRMS = progressive relapsing MS; RMS = relapsing MS; SD = standard deviation; SPMS = secondary progressive MS.

**TABLE 2.** Comparison between controls and RMS and PMS Patients Using Linear Regression with Age and Sex as Covariates

Area	Group	Adj. Mean	SE, Mean	Mean Diff.	SE, Diff.	<i>p</i>	95% Confidence Interval, Diff.	Rater 1: <i>p</i>	Rater 2: <i>p</i>
Mean GM area, mm <sup>2</sup>	Controls	19.63	0.44						
	RMS	18.33	0.21	1.30	0.48	0.008 <sup>a</sup>	0.35 to 2.25	0.012 <sup>a</sup>	0.013 <sup>a</sup>
	PMS	15.24	0.41	3.09	0.47	<0.001 <sup>a</sup>	2.16 to 4.01	<0.001 <sup>a</sup>	<0.001 <sup>a</sup>
Mean WM area, mm <sup>2</sup>	Controls	58.62	1.49						
	RMS	59.32	0.73	-0.70	1.64	0.671	-3.95 to 2.55	0.694	0.655
	PMS	54.63	1.39	4.69	1.59	0.004 <sup>a</sup>	1.54 to 7.84	0.011 <sup>a</sup>	0.001 <sup>a</sup>
UCCA, mm <sup>2</sup>	Controls	78.25	1.82						
	RMS	77.65	0.89	0.60	2.00	0.765	-3.36 to 4.57	0.751	0.780
	PMS	69.88	1.69	7.78	1.94	<0.001 <sup>a</sup>	3.94 to 11.61	<0.001 <sup>a</sup>	<0.001 <sup>a</sup>
GM area/UCCA ratio, %	Controls	25.12	0.37						
	RMS	23.65	0.18	1.46	0.41	<0.001 <sup>a</sup>	0.65 to 2.27	0.001 <sup>a</sup>	0.005 <sup>a</sup>
	PMS	21.79	0.35	1.85	0.40	<0.001 <sup>a</sup>	1.07 to 2.64	<0.001 <sup>a</sup>	0.053

Mean values are least square means with adjustment for age and sex. The 3rd to 8th columns refer to mean values of both raters. The 9th and 10th columns refer to the individual ratings. Mean differences: the first line refers to the difference between controls and RMS, the second line to the difference between RMS and PMS. Controls, n = 20; RMS, n = 88; PMS, n = 25. Probability values are 2-sided.

<sup>a</sup>Statistically significant.

Adj. = adjusted; Diff. = difference between means; GM = gray matter; PMS = progressive multiple sclerosis; RMS = relapsing multiple sclerosis; SE = standard error; UCCA = upper cervical cord area; WM = white matter.

this level is well above the cervical enlargement, which is highly variable anatomically. Therefore, the areas assessed at the C2/C3 disk level yield more reproducible measurements of the cross-sectional cord area.<sup>33</sup> In addition, MRI changes at this segmental level correlate with disability in longstanding MS.<sup>34–36</sup>

Intra-rater and inter-rater reliability for the GM area assessments showed ICCs of 0.98 and 0.91, respectively. The inter-rater ICC for UCCA assessments was >0.99. All statistical differences were quantitatively similar between operators (Tables 2 and 3, Supplementary Table 1).

When adjusted either for age and gender or for disease duration and gender, the mean spinal cord GM, WM, and UCCA areas at C2/C3 were significantly smaller in patients with progressive MS patients compared to RMS patients or compared to those with an apparently mild disease course (see Tables 2 and 3, Supplementary Table 1). Moreover, the percentage reduction of these adjusted GM areas (comparing progressive MS to RMS patients) was more than double the percentage reduction in WM area (17% vs 8%). In addition, patients with progressive MS had a significantly lower ratio of GM area to UCCA (21.8%) compared to patients with RMS (23.7%; *p* < 0.001). Figure 2 shows PSIR images of three RMS and three PMS patients illustrating GM atrophy in progressive MS.

The RMS patients had smaller mean GM areas compared to healthy controls (*p* = 0.008). No significant differences were found for the mean WM areas (*p* = 0.671) and the UCCA (*p* = 0.765) between these groups.

To mitigate potential bias in the segmentation for controls compared to RMS data, one reader (R.S.) performed an additional masked reading of the 20 controls mixed in with 30 randomly selected RMS patients out of a total of 54 RMS patients without visible lesions on the PSIR images. The areas determined from the masked reading were consistent with the original nonmasked readings of the controls (ICC = 0.95). The data obtained in the blinded experiment confirmed the subtle but significant GM differences between controls and RMS patients in regard to both absolute values of spinal cord GM areas and differences in spinal cord GM areas (mean spinal cord GM area difference between controls and RMS = 1.40mm<sup>2</sup>, *p* = 0.003).

The results of the correlation between PSIR and clinical measures are summarized in Table 4. As shown in Figure 3, there was an inverse correlation of spinal cord GM area, WM area, and UCCA area at C2/C3 with the EDSS (Spearman rho: -0.60, -0.32, and -0.42, respectively, all *p* ≤ 0.001) and moreover with the T25W (Spearman rho: -0.50, -0.28, and -0.36;

**TABLE 3. Comparison between Controls and Patients with MMS and PMS Using Linear Regression with Age and Sex as Covariates**

Area	Group	Adj. Mean	SE, Mean	Mean Diff.	SE, Diff.	<i>p</i>	95% Confidence Interval, Diff.	Rater 1: <i>p</i>	Rater 2: <i>p</i>
Mean GM area, mm <sup>2</sup>	Controls	19.47	0.43						
	MMS	18.05	0.35	1.42	0.56	0.013 <sup>a</sup>	0.31 to 2.53	0.035 <sup>a</sup>	0.012 <sup>a</sup>
	PMS	14.99	0.38	3.06	0.51	<0.001 <sup>a</sup>	2.04 to 4.09	<0.001 <sup>a</sup>	<0.001 <sup>a</sup>
Mean WM area, mm <sup>2</sup>	Controls	58.31	1.59						
	MMS	58.55	1.30	0.24	2.07	0.909	-3.88 to 4.36	0.965	0.856
	PMS	53.78	1.39	4.77	1.90	0.014 <sup>a</sup>	0.99 to 8.56	0.039 <sup>a</sup>	0.005 <sup>a</sup>
UCCA, mm <sup>2</sup>	Controls	77.79	1.91						
	MMS	76.61	1.57	1.18	2.48	0.635	-3.76 to 6.13	0.632	0.640
	PMS	68.77	1.66	7.84	2.27	0.001 <sup>a</sup>	3.30 to 12.38	0.001 <sup>a</sup>	0.001 <sup>a</sup>
GM area/UCCA ratio, %	Controls	25.07	0.40						
	MMS	23.65	0.32	1.41	0.51	0.007 <sup>a</sup>	0.39 to 2.43	0.029 <sup>a</sup>	0.013 <sup>a</sup>
	PMS	21.83	0.34	1.83	0.47	<0.001 <sup>a</sup>	0.89 to 2.76	<0.001 <sup>a</sup>	0.237

Mean values are least square means with adjustment for age and sex. The 3rd to 8th columns refer to mean values of both raters. The 9th and 10th columns refer to the individual ratings. Mean differences: the first line refers to the difference between controls and MMS, the second line to the difference between MMS and PMS. Controls, n = 20; MMS (subgroup of RMS), n = 28; PMS, n = 25. Probability values are 2-sided.

<sup>a</sup>Statistically significant.

Adj. = adjusted; Diff. = difference between means; GM = gray matter; MMS = mild multiple sclerosis; PMS = progressive multiple sclerosis; SE = standard error; UCCA = upper cervical cord area; WM = white matter.

$p < 0.001$ ,  $p = 0.004$ ,  $p < 0.001$ , respectively). In addition, the GM area (Spearman rho = -0.37,  $p < 0.001$ ) and the UCCA (rho = -0.22,  $p = 0.024$ ) were significantly negatively correlated with the 9HPT, whereas the WM area was not (Spearman rho = -0.15,  $p = 0.108$ ).

Normalized brain GM volumes and mean spinal cord GM areas were weakly correlated (Pearson rho = 0.25,  $p = 0.008$ ). The number of spinal cord lesions was not correlated with mean spinal cord GM area (Spearman rank rho = -0.11,  $p = 0.273$ ), mean spinal cord WM area (Spearman rank rho = 0.09,  $p = 0.356$ ), or total cord area (Spearman rank rho = 0.05,  $p = 0.618$ ).

Spinal cord GM area was the strongest correlate of EDSS in all LEAPS models independent of size. EDSS scores were largely driven by the variables *spinal cord GM area* and *normalized brain GM volume*, whereas all other variables (brain T1 lesion load, brain FLAIR lesion load, spinal cord WM area, number of spinal cord T2 lesions, normalized brain WM volume, age, disease duration, and sex) made only minor contributions to the variance explained by the model (Table 5, Fig 4). Together these measures accounted for 50.82% of the EDSS variance.

Using bootstrapping, the relative contribution of the variable *spinal cord GM area* to EDSS was shown to be significantly greater than the contribution of the variable *normalized brain WM volume* (CI of the difference of the relative importance between these 2 metrics =

0.1007–0.2889), and than those of the variables *normalized brain GM volume* (CI of the difference = 0.0276–0.2706) and *spinal cord WM area* (CI = 0.0952–0.2559; Supplementary Table 2).

Figure 5A shows the estimated risk of a mild or progressive disease course based on binary logistic regression with either normalized brain GM volume (x-axis) or spinal cord GM area (y-axis) as single predictors. Whereas the model based on brain GM volume alone allows only for assignment of 3 progressive patients as “progressive” with a risk above >0.7, the spinal cord GM area allows for an additional 13 progressive patients to be correctly assigned using the same cutoff. In an analogous way, Figure 5B shows the estimated risk of a relapsing or progressive disease course.

The diagnostic likelihood ratio test confirmed that whereas spinal cord GM area significantly improves the prediction of both progressive versus mild and progressive versus relapsing disease courses while controlling for normalized brain GM volume, the normalized brain GM volume does not significantly improve this prediction when controlling for spinal cord GM areas.

Figure 6A displays the ROC curves for the prediction of a progressive versus relapsing disease course by the binary logistic models with either normalized brain GM volume (gray curve) or spinal cord GM area (black curve) as single predictors or the combination of both

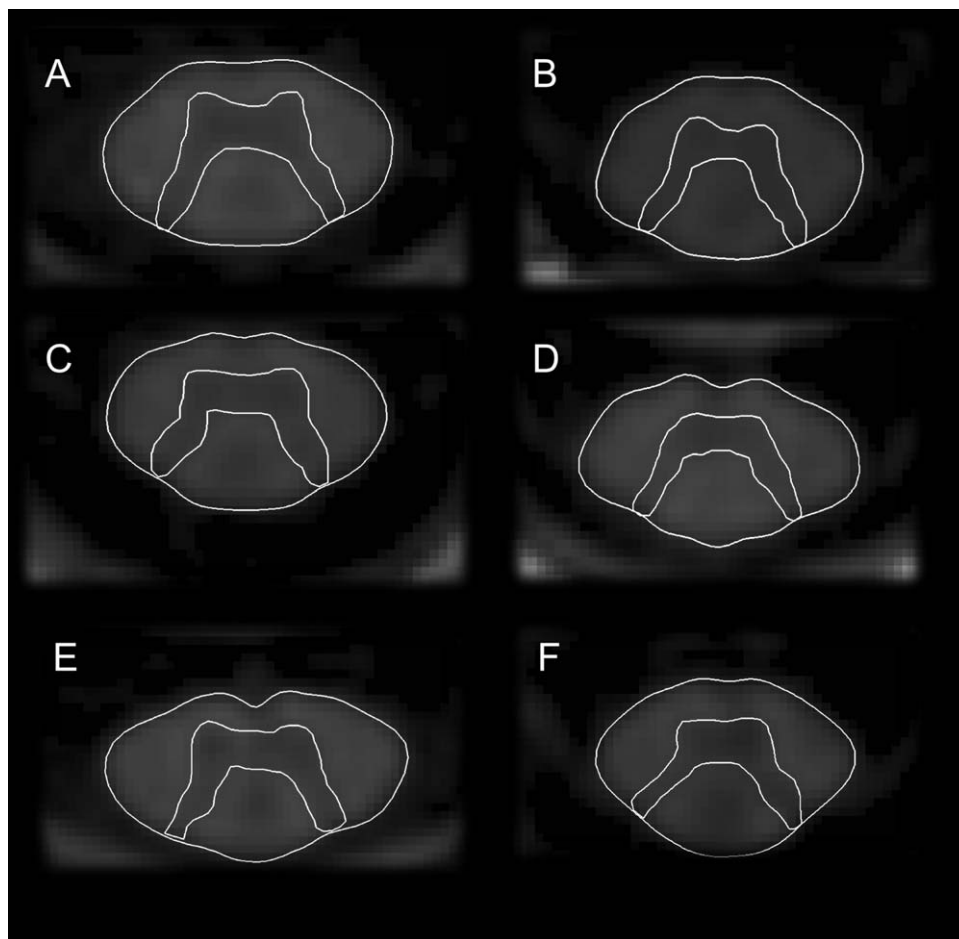


**FIGURE 2:** (A–F) Axial 2-dimensional phase-sensitive inversion images at the C2/C3 disk level of patients with relapsing–remitting multiple sclerosis (MS) and Expanded Disability Status Score < 2.0 (A, C, E) and patients with primary progressive (B) and secondary progressive MS (D, F) illustrating gray matter (GM) atrophy in progressive MS. Notice the selective atrophy of the spinal cord GM in the patient with progressive MS and moderate disability (EDSS = 4.0; B) and both white matter and GM atrophy in severely disabled secondary progressive MS of long disease duration (F).

(dotted curve). The area under the ROC curve was 0.89 for the model based on spinal cord GM area alone, 0.69 for the model based on brain GM volume alone, and 0.90 for the combined model. Figure 6B shows the analogous results for prediction of a progressive versus mild outcome.

## Discussion

The results of this study provide the first reported in vivo evidence of a significant association between the spinal cord GM area and disability and disease type found in MS patients. Both the spinal cord GM and WM areas at the intervertebral disk level of C2/C3 were lower in

**TABLE 4. Spearman Rank Correlations between PSIR and Clinical Measures**

Parameter	Mean WM Area	Mean GM Area	Mean UCCA, C2/C3
EDSS	−0.32, $p = 0.001^a$	−0.60, $p < 0.001^a$	−0.42, $p < 0.001^a$
T25W	−0.28, $p = 0.004^a$	−0.50, $p < 0.001^a$	−0.36, $p < 0.001^a$
9HPT	−0.15, $p = 0.108^a$	−0.37, $p < 0.001^a$	−0.22, $p = 0.024^a$

Spearman rank rho correlation coefficients. PSIR measurements were taken at the C2/C3 disk level; mean spinal cord WM, spinal cord GM and UCCA values of both readers were analyzed.

<sup>a</sup>Statistically significant.

9HPT = 9-Hole Peg Test; EDSS = Expanded Disability Status Score; GM = gray matter; PSIR = phase-sensitive inversion recovery; T25W = Timed 25-Foot Walk Test; UCCA = upper cervical cord area; WM = white matter.

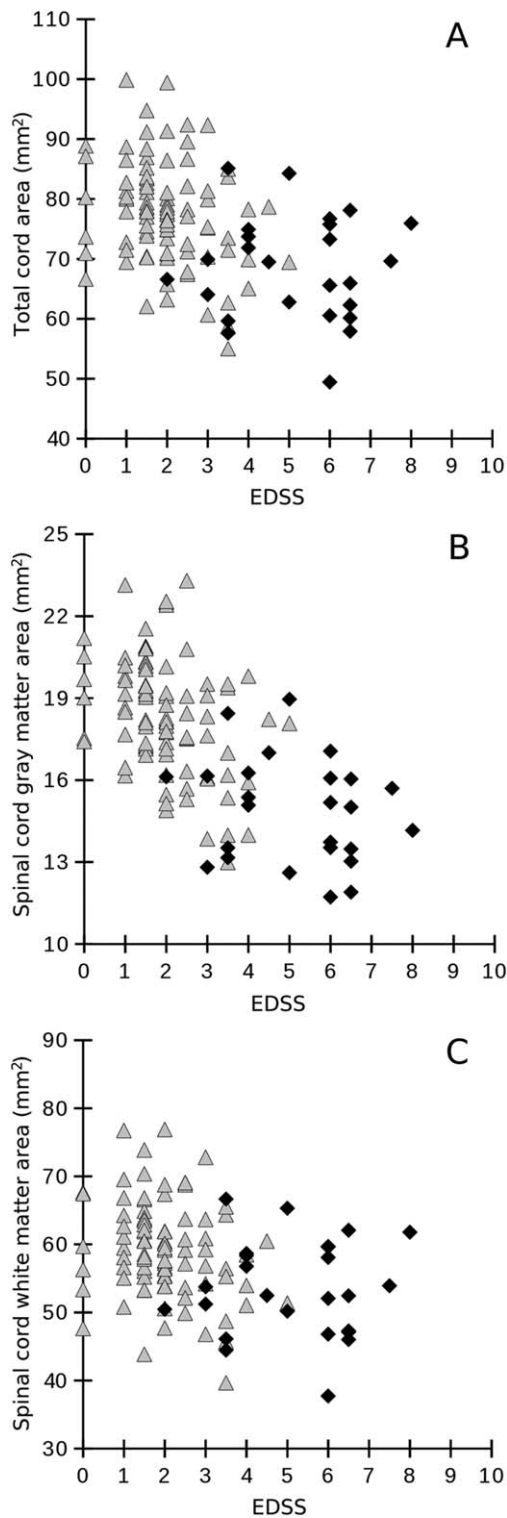


**FIGURE 3:** Associations between the Expanded Disability Status Score (EDSS; x-axis) and (A) total spinal cord area, (B) mean spinal cord gray matter area, and (C) spinal cord white matter area (given in  $\text{mm}^2$ , y-axis) using Spearman rank correlation. Correlation coefficients are as follows: (A)  $\rho = -0.42$ ,  $p < 0.001$ ; (B)  $\rho = -0.60$ ,  $p < 0.001$ ; (C)  $\rho = -0.32$ ,  $p = 0.001$ . Measurements were taken at the C2/C3 intervertebral disk level. White triangles represent relapsing MS patients; black diamonds represent progressive MS patients.

patients with a progressive disease course than in patients with an RMS disease course (adjusted for age and sex) with proportionally more GM than WM atrophy in progressive compared to RMS. These findings suggest that there is a preferential loss of spinal cord GM in progressive MS.

In addition, RMS patients showed significantly smaller spinal cord GM areas than did controls in the absence of significant differences of WM areas and total cord areas, indicating a subtle but selective GM loss already during the relapsing phase. Moreover, the spinal cord GM area was inversely associated with disability as determined by the EDSS and T25W scores, with correlation coefficients of  $-0.60$  and  $-0.50$ , respectively.

The association between spinal cord area measurements and disability was also found within the RMS subgroup, although the correlation was strengthened by the addition of the PMS patients.

Spinal cord GM area was the strongest predictor of disability in a model including normalized brain GM and WM volumes, brain T1 lesion load, spinal cord WM area, and number of spinal cord lesions, underscoring the clinical relevance of these findings.

A reduction in the cross-sectional upper cervical cord area is a well-known finding in MS. Progressive patients and those with higher EDSS scores have smaller areas compared to RMS patients or those with low EDSS scores.<sup>33,35–38</sup> However, until recently, the relative contribution of the WM and GM to this pathological process could only be evaluated in autopsy series, which provided conflicting results. Whereas some histopathological studies<sup>14</sup> found a predominance of spinal cord WM atrophy in MS patients compared to controls, other studies, in particular autopsy studies conducted soon after death,<sup>13</sup> found no significant difference between the reductions in GM and WM area in advanced progressive MS patients.

Autopsy-based studies have several inherent limitations. Well-known confounders include variability in the timing of death, autopsy, and commencement of fixation. Furthermore, postmortem volumetric assessments of central nervous system structure are subject to fixation effects that can result in unpredictable swelling, shrinkage, or brain deformation.<sup>39</sup> Several authors tried to account for fixation-related shrinkage in the spinal cord by applying a general correction factor.<sup>14,40</sup> However, the comparison between the spinal cord mean GM and WM areas in controls without spinal cord disease measured postmortem at the C3 segmental level<sup>41</sup> and our results revealed a striking compartment-related difference. Whereas the postmortem spinal cord and WM areas were reduced by 33% and 22% of the in vivo

**TABLE 5. LMG Estimation of the Relative Contributions of Variables to the Linear Regression Model with Expanded Disability Status Score as the Dependent Variable,  $R^2 = 0.5082$**

Variable	Relative Importance Metrics, Normalized to Sum to 100%	Relative Importance Metrics, Non-normalized	95% CI of the Non-normalized Relative Importance Metrics
Mean spinal cord GM area	0.4609	0.2342	0.1529–0.3149
Mean spinal cord WM area	0.1005	0.0511	0.0233–0.1021
Number of spinal cord T2 lesions	0.0335	0.0170	0.0022–0.0634
Normalized brain GM volume	0.1414	0.0719	0.0211–0.1537
Normalized brain WM volume	0.0660	0.0335	0.0181–0.0627
Brain T1 lesion volume	0.0844	0.0429	0.0063–0.1174
Brain FLAIR lesion volume	0.0430	0.0219	0.0035–0.0627
Sex	0.0073	0.0037	0.0012–0.0366
Age	0.0351	0.0179	0.0059–0.0666
Disease duration	0.0279	0.0142	0.0064–0.0403

The following variables significantly contribute to the multivariate model: spinal cord GM and WM areas, normalized brain GM and WM volumes, brain T1 lesion volume, brain FLAIR lesion volume, number of spinal cord T2 lesions, age, disease duration, and sex.  
 CI = confidence interval, determined using Bootstrapping (1,000 iterations); FLAIR = fluid-attenuated inversion recovery; GM = gray matter; WM = white matter.

measurements, respectively, the GM areas were disproportionately reduced by 63%. A pronounced fixation-related shrinkage of brain GM compared to WM was previously described.<sup>42</sup> Importantly, fixation effects on

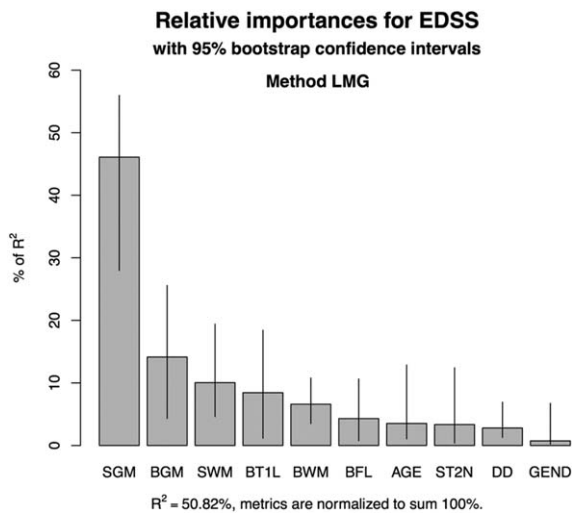


**FIGURE 4: Relative contributions of the variables to the Expanded Disability Status Score (EDSS) using a LEAPS model. AGE = age; BFL = brain fluid-attenuated inversion recovery lesion volume; BGM = normalized brain gray matter volume; BT1L = brain T1 lesion volume; BWM = normalized brain white matter volume; DD = disease duration; GEND = gender; SGM = spinal cord gray matter area; ST2N = spinal cord T2 lesion number; SWM = spinal cord white matter area.**

spinal cord WM and GM volumes in MS-affected (eg, gliotic) tissue have not been determined. Potential differences between these tissues have to be considered when interpreting the aforementioned volumetric postmortem studies in MS.

We present in vivo cervical spinal cord area data from a large cohort of relapsing and progressive MS patients that discriminate spinal cord GM and WM signals within the cord using SF-SIGMA. Our results indicate that, even in the absence of WM loss, there is a detectable loss of tissue in the GM in relapsing MS that is more prominent during the progressive phase of the illness. Calculating the GM to total cord area ratios from the raw data reported in the autopsy series by Bjartmar et al<sup>13</sup> reveals a trend toward a greater GM reduction in the cervical spinal cord in progressive patients compared to controls (GM to total cord area ratio of 22.4% in 6 controls vs 20.2% in 5 progressive MS cases). These proportions are similar to our MRI-based observations.

For decades, MS has been regarded as the prototypical autoimmune-mediated central nervous system WM disease. Our results indicate that MS disability is, among different MRI measures, predominantly explained by indicators of GM disease, with indicators of WM disease having a relatively minor impact on the variance explained by linear regression modeling.

Many groups have documented brain GM atrophy throughout the disease course.<sup>43–48</sup> Cortical atrophy

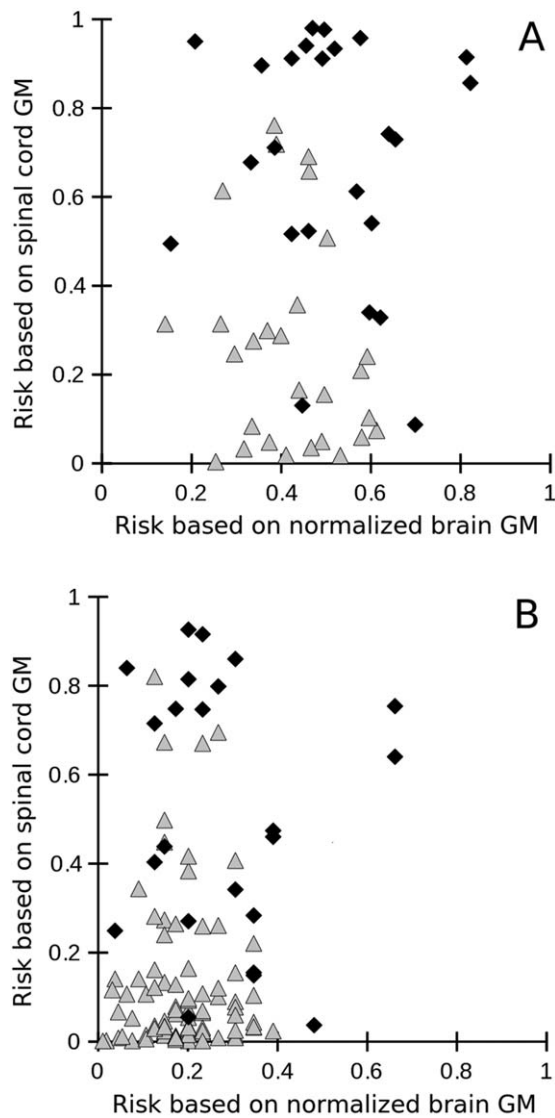


**FIGURE 5:** Estimated risk of having (A) a progressive (1) versus mild disease course (0) or (B) a progressive (1) versus relapsing (0) disease course using binary logistic regression based on either normalized brain gray matter (GM) volume alone (x-axis) or spinal cord GM area (y-axis). Progressive patients are represented by black diamonds; patients with a relapsing or mild course are represented by gray triangles.

correlates with cognitive impairment<sup>49,50</sup> and disability,<sup>47,51–53</sup> accelerates with disease stage,<sup>54</sup> and evolves faster in patients with progressive disease compared to stable patients.<sup>55</sup> The underlying pathological mechanisms leading to cortical thinning are not fully understood. Nevertheless, *in vivo* cortical and subcortical GM atrophy is thought to reflect a combination of demyelination, axonal, and dendritic transections, apoptotic loss of neurons, and reduced synaptic or glial densities.<sup>7,10,56,57</sup>

The *in vivo* reductions in spinal cord GM area that we observed are probably due in part to a loss of neurons in the cervical spinal cord (as has been described in histopathological studies<sup>12</sup>) and also likely reflect changes to

the neuropil.<sup>57</sup> The extent of demyelination in the spinal cord GM greatly exceeds that of the spinal cord WM or cortex.<sup>11</sup> The relatively poor correlations between spinal cord GM area and normalized brain GM volume we found suggest that the processes underlying atrophy of the brain GM and of spinal cord GM might proceed independently or reflect different pathophysiological manifestations of the disease. The absence of a correlation between spinal cord lesions and spinal cord atrophy is consistent with imaging findings by Lukas et al.<sup>58</sup> and Rocca et al.,<sup>38</sup> and with histopathological data by

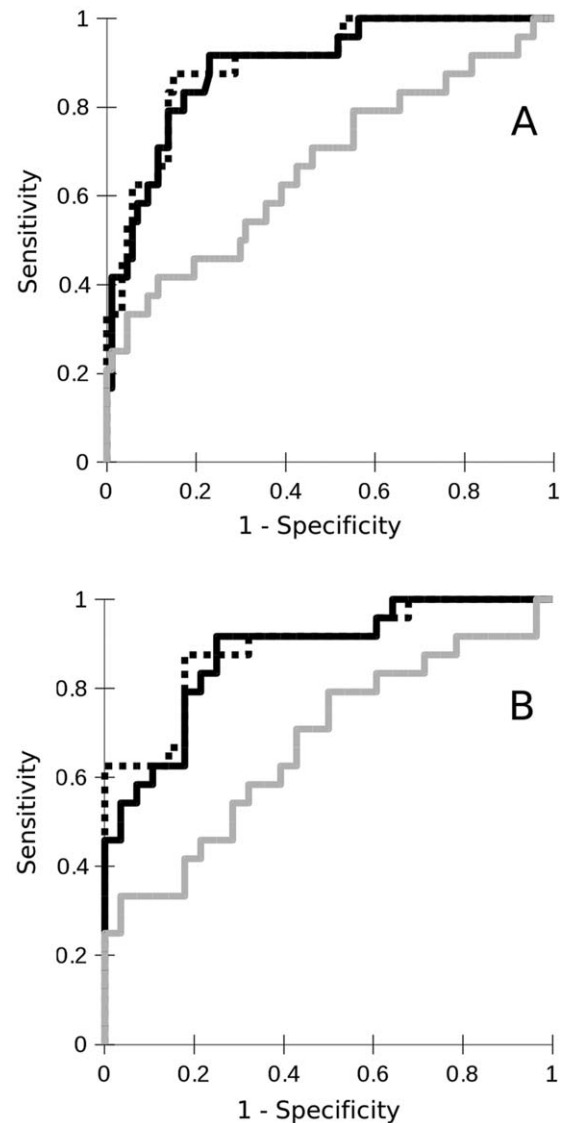


**FIGURE 6:** Receiver operating characteristic curve displaying the sensitivities and specificities to classify (A) a progressive versus relapsing disease course and (B) a progressive versus mild disease course based on binary logistic models based on either brain gray matter (GM) volume (gray curve) or spinal cord GM area (black curve) or both (dotted line). The areas under the curve were (A) 0.69, 0.89, and 0.90, respectively and (B) 0.67, 0.88, and 0.89, respectively.

Evangelou et al,<sup>40</sup> suggesting that spinal cord atrophy is largely independent of tissue loss within lesions.

Our study has a number of limitations that should be considered in interpreting the results. First, the GM area segmentation was performed manually and could result in operator-dependent bias (a fully automated segmentation method is not available). To account for this possible source of bias, we used 2 independent raters, who were masked to clinical assessments. The inter-rater reliability of GM area assessments was excellent (ICC = 0.91), suggesting that different raters can reliably assess GM matter segmentation. Second, delimitation of the spinal cord GM at C2/C3 was only possible in a subset of the patients who underwent MRI (113 of 127 MS patients or 89%). Given that assessments were performed in nearly 90% of evaluable scans, we believe that the results reported are representative of the overall data set. That said, a reason for difficulty in delimiting spinal cord GM at C2/C3 was the extent of lesions present at this level that obfuscate distinction between GM and WM structure. It is possible that these lesions could have an impact on either GM or WM area, and therefore the direction of this potential source of bias is difficult to estimate.

Finally, this is a cross-sectional study. Longitudinal association between cord GM changes and clinical progression remains to be determined. By their nature, cross-sectional studies cannot be used to determine cause-effect relationships, so we are not able to determine whether spinal cord GM atrophy precedes or coincides with MS-related disability. Nevertheless, we believe that the comparisons of relapsing or apparently mild MS with progressive MS and with healthy controls are valid and welcome replication of our observations by other groups who are technologically similarly equipped. In this regard, we found that the main advantage of SF-SIGMA in comparison to the protocols based on the higher-resolution 3D PSIR sequence with larger coverage<sup>20,21</sup> is the relatively short acquisition time of <2 minutes, which enhances applicability to larger cohorts.

In conclusion, our study provides the first in vivo evidence of the clinical relevance of spinal cord GM atrophy in MS. Upper cervical GM areas were reduced in the absence of spinal cord WM atrophy in RMS, and GM atrophy was substantially more pronounced in progressive MS compared to RMS patients or to those with mild disease courses. Moreover, independently from brain GM atrophy, spinal cord GM area correlated with disability. The validity of spinal cord GM area assessments as a potential predictor of progression will need to be determined in longitudinal studies.

## Acknowledgment

This study was supported by a gift from the Ostby Foundation (R.G.H.), and research grant funding from the

National Multiple Sclerosis Society; Conrad H. Hilton Foundation; Department of Defense; NIH R01 NS 026799, R01 NS049477, and K02 NS072288; National Defense Science and Engineering Fellowship (K.M.J.); and Nancy Davis Foundation. R.S. has received grants from the Swiss MS Society and the Gottfried and Julia Bangerter-Rhyner Foundation, Switzerland.

We thank R. Gomez, C. Ciocca, R. Kanner, A. Evangelista, B. Amirbekian, and A. Santaniello for help with data acquisition and/or data management.

## Potential Conflicts of Interest

J.M.G.: grant, National MS Society, NIH National Center for Advancing Translational Sciences (KL2TR000143); personal fees, National MS Society, Medical-Legal Consulting. A.J.G.: personal fees, Applied Clinical Intelligence/Biogen, Medimmune, Novartis, Roche, Mylan, Bionure; grant, National MS Society, HHMI, UCSF CTSI. K.M.J.: NDSEG fellowship award, Department of Defense. H.-C.v.B.: grant, Roche, Genzyme, Pfizer; personal fees, Novartis. B.A.C.C.: consultancy, Abbvie, Biogen Idec, EMD Serono, Genzyme/Sanofi-Aventis, Medimmune, Novartis, Teva Neurosciences; grant, Hoffman La Roche. S.L.H.: personal fees, BioMarin, Receptos, Symbiotix, Annexon. R.G.H.: grant, Stem Cells Inc, Roche; personal fees, Stem Cells Inc, Novartis.

## References

- Dejerine J. Etude sur la sclérose en plaques cérébrospinale à forme de sclérose latérale amyotrophique. *Rev Med* 1884;4:193.
- Brauer L. Muskelatrophie bei multipler Sklerose. *Neurol Centralbl* 1898;17:635.
- Bouchaud. Sclérose en plaques avec amyotrophique. *J Neurol* 1900;5:348.
- Lejonne MP. Contribution à l'étude des atrophies musculaires dans la sclérose en plaques. Paris, France: G. Steinheil, 1903.
- Davison C, Goodhart SP, Lander J. Multiple sclerosis and amyotrophies. *Arch Neurol Psychiatry* 1934;31:270-289.
- Dawson JW. The histology of multiple sclerosis. *Trans R Soc Edinburgh* 1916;50:517-740.
- Peterson JW, Bö L, Mörk S, et al. Transected neurites, apoptotic neurons, and reduced inflammation in cortical multiple sclerosis lesions. *Ann Neurol* 2001;50:389-400.
- Bø L, Vedeler CA, Nyland HI, et al. Subpial demyelination in the cerebral cortex of multiple sclerosis patients. *J Neuropathol Exp Neurol* 2003;62:723-732.
- Kutzelnigg A, Lucchinetti CF, Stadelmann C, et al. Cortical demyelination and diffuse white matter injury in multiple sclerosis. *Brain* 2005;128:2705-2712.
- Geurts JJ, Calabrese M, Fisher E, Rudick RA. Measurement and clinical effect of grey matter pathology in multiple sclerosis. *Lancet Neurol* 2012;11:1082-1092.
- Gilmore CP, Donaldson I, Bö L, et al. Regional variations in the extent and pattern of grey matter demyelination in multiple

- sclerosis: a comparison between the cerebral cortex, cerebellar cortex, deep grey matter nuclei and the spinal cord. *J Neurol Neurosurg Psychiatry* 2009;80:182–187.
12. Gilmore CP, DeLuca GC, Bö L, et al. Spinal cord neuronal pathology in multiple sclerosis. *Brain Pathol* 2009;19:642–649.
  13. Bjartmar C, Kidd G, Mörk S, et al. Neurological disability correlates with spinal cord axonal loss and reduced N-acetyl aspartate in chronic multiple sclerosis patients. *Ann Neurol* 2000;48:893–901.
  14. Gilmore CP, DeLuca GC, Bö L, et al. Spinal cord atrophy in multiple sclerosis caused by white matter volume loss. *Arch Neurol* 2005;62:1859–1862.
  15. Dietrich O, Reiser MF, Schoenberg SO. Artifacts in 3-T MRI: physical background and reduction strategies. *Eur J Radiol* 2008;65:29–35.
  16. Yiannakas MC, Kearney H, Samson RS, et al. Feasibility of grey matter and white matter segmentation of the upper cervical cord in vivo: a pilot study with application to magnetisation transfer measurements. *Neuroimage* 2012;63:1054–1059.
  17. Taso M, Le Troter A, Sdika M, et al. Construction of an in vivo human spinal cord atlas based on high-resolution MR images at cervical and thoracic levels: preliminary results. *MAGMA* 2014;27:257–267.
  18. Kellman P, Arai AE, McVeigh ER, Aletras AH. Phase-sensitive inversion recovery for detecting myocardial infarction using gadolinium-delayed hyperenhancement. *Magn Reson Med* 2002;47:372–383.
  19. Huber AM, Schoenberg SO, Hayes C, et al. Phase-sensitive inversion-recovery MR imaging in the detection of myocardial infarction. *Radiology* 2005;237:854–860.
  20. Kearney H, Miszkil KA, Yiannakas MC, et al. A pilot study of white and grey matter involvement by multiple sclerosis spinal cord lesions. *Mult Scler Relat Disord* 2013;2:103–108.
  21. Kearney H, Yiannakas MC, Abdel-Aziz K, et al. Improved MRI quantification of spinal cord atrophy in multiple sclerosis. *J Magn Reson Imaging* 2014;39:617–623.
  22. Papinutto N, Panara V, Ahn S, et al. Phase sensitive inversion recovery imaging of the spinal cord in clinical scan times. Paper presented at: ISMRM-ESMRMB Joint Annual Meeting; May 10–16, 2014; Milan, Italy.
  23. Polman CH, Reingold SC, Banwell B, et al. Diagnostic criteria for multiple sclerosis: 2010 revisions to the McDonald criteria. *Ann Neurol* 2011;69:292–302.
  24. Kurtzke JF. Rating neurologic impairment in multiple sclerosis: an expanded disability status scale (EDSS). *Neurology* 1983;33:1444–1452.
  25. Kappos L, Lechner-Scott J, Wu S. Neurostatus.net: independent internet platform for training and certification of physicians participating in projects that use a standardised, quantified neurological examination and assessment of Kurtzke's Functional Systems and Expanded Disability Status Scale in Multiple Sclerosis. September 2008 version. Available at: <http://www.neurostatus.net>. Accessed October 31, 2013.
  26. Fischer JS, Rudick RA, Cutter GR, Reingold SC. The Multiple Sclerosis Functional Composite Measure (MSFC): an integrated approach to MS clinical outcome assessment. National MS Society Clinical Outcomes Assessment Task Force. *Mult Scler* 1999;5:244–250.
  27. Horsfield MA, Sala S, Neema M, et al. Rapid semi-automatic segmentation of the spinal cord from magnetic resonance images: application in multiple sclerosis. *Neuroimage* 2010;50:446–455.
  28. Lublin F, Reingold S. Defining the clinical course of multiple sclerosis: results of an international survey. *Neurology* 1996;46:907–911.
  29. Miller AJ. *Subset selection in regression*. 2nd ed. New York, NY: Chapman & Hall/CRC, 2002.
  30. Genizi A. Decomposition of R<sup>2</sup> in multiple regression with correlated regressors. *Stat Sin* 1993;3:407–420.
  31. Groemping U. Relative importance for linear regression in R: the package relaimpo. *J Stat Softw* 2006;17(1).
  32. Gu W, Pepe MS. Estimating the capacity for improvement in risk prediction with a marker. *Biostatistics* 2009;10:172–186.
  33. Losseff NA, Webb SL, O'Riordan JI, et al. Spinal cord atrophy and disability in multiple sclerosis. A new reproducible and sensitive MRI method with potential to monitor disease progression. *Brain* 1996;119:701–708.
  34. Furby J, Hayton T, Anderson V, et al. Magnetic resonance imaging measures of brain and spinal cord atrophy correlate with clinical impairment in secondary progressive multiple sclerosis. *Mult Scler* 2008;14:1068–1075.
  35. Bonati U, Fisniku LK, Altmann DR, et al. Cervical cord and brain grey matter atrophy independently associate with long-term MS disability. *J Neurol Neurosurg Psychiatry* 2011;82:471–472.
  36. Kearney H, Rocca MA, Valsasina P, et al. Magnetic resonance imaging correlates of physical disability in relapse onset multiple sclerosis of long disease duration. *Mult Scler* 2014;20:72–80.
  37. Bieniek M, Altmann DR, Davies GR, et al. Cord atrophy separates early primary progressive and relapsing remitting multiple sclerosis. *J Neurol Neurosurg Psychiatry* 2006;77:1036–1039.
  38. Rocca MA, Horsfield MA, Sala S, et al. A multicenter assessment of cervical cord atrophy among MS clinical phenotypes. *Neurology* 2011;76:2096–2102.
  39. Grinberg LT, Amaro E Jr, Teipel S, et al. Brazilian Aging Brain Study Group. Assessment of factors that confound MRI and neuropathological correlation of human postmortem brain tissue. *Cell Tissue Bank* 2008;9:195–203.
  40. Evangelou N, DeLuca GC, Owens T, Esiri MM. Pathological study of spinal cord atrophy in multiple sclerosis suggests limited role of local lesions. *Brain* 2005;128:29–34.
  41. Kameyama T, Hashizume Y, Sobue G. Morphologic features of the normal human cadaveric spinal cord. *Spine* 1996;21:1285–1290.
  42. Kretschmann HJ, Tafesse U, Herrmann A. Different volume changes of cerebral cortex and white matter during histological preparation. *Microsc Acta* 1982;86:13–24.
  43. Miller DH, Barkhof F, Frank JA, et al. Measurement of atrophy in multiple sclerosis: pathological basis, methodological aspects and clinical relevance. *Brain* 2002;125:1676–1695.
  44. Dalton CM, Chard DT, Davies GR, et al. Early development of multiple sclerosis is associated with progressive grey matter atrophy in patients presenting with clinically isolated syndromes. *Brain* 2004;127:1101–1107.
  45. Calabrese M, Rinaldi F, Mattisi I, et al. The predictive value of gray matter atrophy in clinically isolated syndromes. *Neurology* 2011;77:257–263.
  46. Tiberio M, Chard DT, Altmann DR, et al. Gray and white matter volume changes in early RRMS: a 2-year longitudinal study. *Neurology* 2005;64:1001–1007.
  47. Fisniku LK, Chard DT, Jackson JS, et al. Gray matter atrophy is related to long-term disability in multiple sclerosis. *Ann Neurol* 2008;64:247–254.
  48. Ceccarelli A, Rocca MA, Pagani E, et al. A voxel-based morphometry study of grey matter loss in MS patients with different clinical phenotypes. *Neuroimage* 2008;42:315–322.
  49. Amato MP, Bartolozzi ML, Zipoli V, et al. Neocortical volume decrease in relapsing-remitting MS patients with mild cognitive impairment. *Neurology* 2004;63:89–93.
  50. Riccitelli G, Rocca MA, Pagani E, et al. Cognitive impairment in multiple sclerosis is associated to different patterns of gray matter atrophy according to clinical phenotype. *Hum Brain Mapp* 2011;32:1535–1543.

51. De Stefano N, Matthews PM, Filippi M, et al. Evidence of early cortical atrophy in MS: relevance to white matter changes and disability. *Neurology* 2003;60:1157–1162.
52. Tedeschi G, Lavorgna L, Russo P, et al. Brain atrophy and lesion load in a large population of patients with multiple sclerosis. *Neurology* 2005;65:280–285.
53. Roosendaal SD, Bendfeldt K, Vrenken H, et al. Grey matter volume in a large cohort of MS patients: relation to MRI parameters and disability. *Mult Scler* 2011;17:1098–1106.
54. Fisher E, Lee JC, Nakamura K, Rudick RA. Gray matter atrophy in multiple sclerosis: a longitudinal study. *Ann Neurol* 2008;64:255–265.
55. Chen JT, Narayanan S, Collins DL, et al. Relating neocortical pathology to disability progression in multiple sclerosis using MRI. *Neuroimage* 2004;23:1168–1175.
56. Dutta R, Chang A, Doud MK, et al. Demyelination causes synaptic alterations in hippocampi from multiple sclerosis patients. *Ann Neurol* 2011;69:445–454.
57. Wegner C, Esiri MM, Chance SA, et al. Neocortical neuronal, synaptic, and glial loss in multiple sclerosis. *Neurology* 2006;67:960–967.
58. Lukas C, Sombekke MH, Bellenberg B, et al. Relevance of spinal cord abnormalities to clinical disability in multiple sclerosis: MR imaging findings in a large cohort of patients. *Radiology* 2013; 269:542–552.